ACS APPLIED MATERIALS & INTERFACES

RESEARCH ARTICLE

www.acsami.org

Real-Time Quantification of Microscale Bioadhesion Events In situ Using Imaging Surface Plasmon Resonance (iSPR)

Nick Aldred,[†] Tobias Ekblad,[‡] Olof Andersson,[‡] Bo Liedberg,[‡] and Anthony S. Clare*[,†]

[†]School of Marine Science and Technology, Newcastle University, Newcastle upon Tyne, NE1 7RU, United Kingdom

[‡]Division of Molecular Physics, Department of Physics, Chemistry and Biology, Linköping University, Linköping SE-581 83, Sweden

ABSTRACT: From macro- to nanoscales, adhesion phenomena are all-pervasive in nature yet remain poorly understood. In recent years, studies of biological adhesion mechanisms, terrestrial and marine, have provided inspiration for "biomimetic" adhesion strategies and important insights for the development of fouling-resistant materials. Although the focus of most contemporary bioadhesion research is on large organisms such as marine mussels, insects and geckos, adhesion events on the micro/nanoscale are critical to our understanding of important underlying mechanisms. Observing and quantifying adhesion at this scale is particularly relevant for the development of biomedical implants and in the prevention of marine biofouling. However, such characterization has so far been restricted by insufficient quantities of material for biochemical analysis and the limitations of contemporary imaging techniques. Here, we introduce a recently developed optical method that allows precise determination of adhesive deposition by microscale organisms in situ and in real time; a capability not before demonstrated. In this extended study we used the cypris larvae of barnacles and a combination of conventional and imaging surface plasmon resonance techniques to observe and quantify adhesive deposition onto a range of model surfaces (CH_3-, COOH-, NH_3-, and mPEG-terminated SAMs and a PEGMA/HEMA hydrogel). We then correlated this deposition to passive adsorption of a putatively adhesive protein from barnacles. In this way, we were able to rank surfaces in order of effectiveness for preventing barnacle cyprid exploration and demonstrate the importance of observing the natural process of adhesion, rather than predicting surface effects from a model system. As well as contributing fundamentally to the knowledge on the adhesion and adhesives of barnacle larvae, a potential target for future biomimetic glues, this method also provides a versatile technique for laboratory testing of fouling-resistant chemistries.

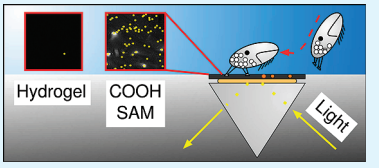

KEYWORDS: imaging SPR, barnacle cyprid, footprints, biological adhesion, biofouling

INTRODUCTION

Recent advances in our understanding of natural biological adhesives have, by necessity, been heavily influenced by the attachment mechanisms of organisms large enough to permit convenient investigation. These have so far included insects,[1] geckos,[2] and the adults of some large marine invertebrates such as barnacles,[3] tubeworms,[4] and mussels[5]. Most analytical methods typically applied to understanding adhesion phenomena, however, are impractical for use with organisms below the millimeter scale, such as the larvae of marine invertebrates. This is because measurement of individual attachment tenacity, direct observation of adhesion in situ and biochemical analysis are challenging for the adhesives of very small or soft-bodied organisms. As well as the difficulties associated with scale and obtaining material for analysis, adhesive processes in natural systems often occur with great speed. Very few contemporary analytical techniques are therefore applicable to the investigation of microadhesion events.

Bioadhesives from fouling organisms are usually transparent when secreted and need to be stained for light microscopy.[6,7] High-resolution observation is limited to a small number of other well-established microscopy techniques. Scanning electron microscopy (SEM) has been the primary tool employed by researchers, but has significant limitations in the present context. Most importantly, samples prepared for observation under conventional SEM must be fixed and dehydrated. Water can be an important component of natural bioadhesives[8] and dehydration certainly alters their appearance substantially.[9] SEM preparation precludes the natural behavior of bioadhesives and observations of real-time adhesive interactions under SEM are impossible. Environmental SEM (ESEM) offers some benefits over conventional SEM, insofar as dehydration and gold coating prior to observation are not strictly required.[10] Unfortunately though, the fine structures present in many biological samples are often not preserved during ESEM.

Although scanning probe microscopy (SPM) has been applied routinely to the study of adhesion at the nanoscale, and has provided valuable fundamental information for the adhesives of fouling invertebrates[11−15] and algae,[9,16−20] the practicalities of this approach with heterogeneous biological materials, and the necessity for replication in all biological studies, compromise the real-world significance of SPM-derived data. Other techniques, such as imaging confocal Raman spectroscopy, may be useful for characterizing the chemical nature of bioadhesives, as was recently shown by Schmidt et al.[21] for barnacle cyprid permanent cement. However, the disadvantage shared by all of these methods when applied to the study of bioadhesion, is their inability to observe large-scale dynamic processes, such as the attachment of an organism or a limb to a surface, in real time.

Received: March 11, 2011
Accepted: May 19, 2011
Published: May 19, 2011

ACS Publications © 2011 American Chemical Society

dx.doi.org/10.1021/am2003075 | *ACS Appl. Mater. Interfaces* 2011, 3, 2085–2091

Table 1. Chemistries of the Test Surfaces Used in SPR/iSPR Experiments

abbreviation	chemistry	surface functional group(s)
CH_3	$HS(CH_2)_{15}CH_3$	methyl
COOH	$HS(CH_2)_{15}COOH$	carboxyl
NH_2	$HS(CH_2)_{11}NH_2 \cdot HCl$	amine
mPEG	$HS(CH_2)_{11}CONH(C_2H_4O)_{11}CH_3$	methoxy-terminated PEG
hydrogel	$PEG_{10}MA/HEMA$	hydrogel with PEG and hydroxyl

These limitations also apply to common optical methods such as laser confocal microscopy and total internal reflection fluorescence microscopy, which usually require fluorescent labeling. Developing methods to facilitate observation of adhesion processes at the micro/nanoscale is nevertheless important, with potential to inspire novel adhesives for specialist purposes and directly benefit the development of fouling-resistant materials for biomedical and marine applications.

With these applications in mind, we developed a protocol for imaging and quantifying adhesion events between microscale organisms and a range of model surfaces using both conventional and imaging surface plasmon resonance (iSPR). To the best of the authors' knowledge, this method is currently unique in its ability to provide quantitative data on the interactions of microfouling organisms with surfaces in situ and in real time.

In the marine environment, colonization of surfaces is initiated by the settlement and adhesion of microscopic spores or larvae. Most benthic invertebrate larvae attach to surfaces using proteinaceous adhesives, however investigations of these adhesives using modern analytical methods have been limited.[12,14,15,21−23] As well as organisms that stick permanently to surfaces, there are also temporary adhesion mechanisms that are of considerable interest. One of these is the temporary adhesion of barnacle cypris larvae.[24] Cyprids, the settling-stage larvae of barnacles, are able to explore immersed surfaces using a rapidly reversible adhesion mechanism mediated by a combination of "hairy footpads" and a viscous proteinaceous material, secreted onto the surface of their attachment discs. Cyprids of the barnacle *Semibalanus balanoides* are approximately 1 mm in length and use their temporary attachment capability to explore immersed surfaces before committing to permanent settlement and metamorphosis into the adult form.[6,25] The ∼30−50 μm diameter (depending on species) attachment discs are located on the third segments of paired antennules[26] at the anterior end of the cyprid, and although cyprid temporary adhesion is not fully understood, it is believed that voluntary attachment and detachment require a combination of both the secreted proteinaceous material and a complex surface structure on the attachment discs. The cyprid temporary adhesion mechanism is highly effective, allowing exploring cyprids to walk across immersed surfaces rapidly (∼2 body-lengths per second) in a bipedal fashion and with tenacity of <0.3 MPa.[27]

During exploration of surfaces, cyprids may deposit trails of "footprints" of the proteinaceous material[28,29] used in adhesion. These footprints appear to be deposited more often on some materials than others,[13,14] but until recently,[30] evidence for this was anecdotal. The exact composition of the footprint material remains unconfirmed for the reasons outlined above; however, there is evidence that the footprints contain, as a major constituent, the barnacle settlement-inducing protein complex (SIPC),[29] a large cuticular glycoprotein found in barnacles and their larvae.[31−33]

Through a combination of conventional and imaging SPR, as developed and described in detail by Andersson et al.,[30] we observed and quantified the deposition of cyprid temporary adhesive material to various model surfaces commonly used in antibiofouling research. By expressing footprint deposition as a frequency of total attempts, and by correlating these data to passive adsorption of a putative adhesive protein from barnacles (SIPC) to the same surfaces, we were able to demonstrate both the efficacy of a powerful method for use in bioadhesion/antifouling research and also the importance of conducting studies of bioadhesion processes within the natural system of interest, rather than by proxy. The results of such studies may serve as inspiration not only for the commercial development of novel glues[34−36] but also for the development of biofouling-resistant coatings[37] for ships and other man-made marine structures.

METHODS

Cyprid Collection. Cyprids of the acorn barnacle, *Semibalanus balanoides,* were collected by plankton tow at Cullercoats, UK (55.18 N, 1. 268 W) during April 2009. They were stored (1 cyprid mL^{-1}) in a 1 L glass bottle (Schott, Duran) containing 33 PSU artificial seawater (ASW; Tropic Marin) at 6 °C prior to use. Cyprids were raised to room temperature (∼23 °C) gradually before use in experiments.

Extraction and Purification of SIPC. SIPC purification followed the protocol of Matsumura et al.[28] Briefly, adult *S. balanoides* were collected from the shore at Cullercoats, North-East England. They were then quickly homogenized and the crude protein extract, buffered throughout at pH 7.5, was subjected to salt precipitation and dialysis. Following dialysis, the crude extract was purified further using ion exchange and size exclusion chromatography. After each step, relevant fractions were identified by Western blotting of a representative sample using an antibody specific to a 76 kDa subunit of the SIPC.

Surface Preparation. Four types of self-assembled monolayers (SAMs) and an ultrathin hydrogel coating were selected as test surfaces for the SPR experiments. The surfaces were prepared as follows: 12 × 12 mm^2 glass slides, coated with a 45 nm thick layer of gold (acquired from GE Healthcare, Biacore division, Uppsala, Sweden), were washed in a 5:1:1 mixture of Milli-Q water, 30% hydrogen peroxide and 25% ammonia (TL-1) at 85 °C for 5 min. The slides were rinsed with water and ethanol and placed in thiol solutions overnight prior to testing. The following thiols were used: $HS(CH_2)_{15}CH_3$ (Fluka, Germany), $HS(CH_2)_{15}COOH$ (Sigma-Aldrich, Germany), $HS(CH_2)_{11}NH_2 \cdot HCl$ (Prochimia, Poland) and $HS(CH_2)_{11}CONH(C_2H_4O)_{11}CH_3$ (mPEG, Polypure AS, Norway). These surfaces are hereafter described as CH_3, COOH, NH_2 and mPEG respectively, as presented in Table 1. The solvent for the incubation solutions was 99.5% pure ethanol in all cases except NH_2, for which Milli-Q water was used. The thiol concentration was 100 μM in all cases.

The hydrogel coating (Table 1) was included in the study because it had previously been shown to limit barnacle settlement significantly,[38] and is known to exhibit very low protein adsorption. The preparation of this surface has been described in detail elsewhere.[38,39] Briefly,

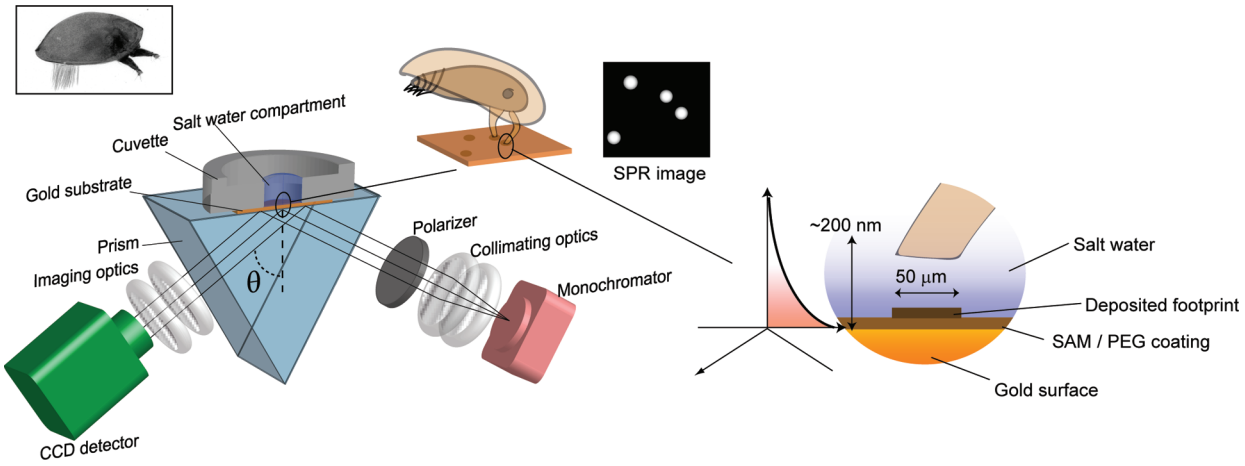

Figure 1. Cartoon of the iSPR experimental setup with the principal components indicated. The cyprid's antennules are visible in the SPR image when they are within the extension of the evanescent field (a few hundred nanometers), as shown schematically in the rightmost magnified view. Deposited footprints are also directly visible in the image and the amount of material in each footprint can be quantified by scanning the wavelength and determining the SPR conditions for each region of the image.

gold-coated glass slides were first coated with mPEG SAMs, as described above. The SAM served as an adhesion layer for the subsequent modification, which was carried out by UV-initiated photografting from an aqueous solution containing 120 mM 2-hydroxyethyl methacrylate (HEMA; Fluka, Germany) and 120 mM polyethylene glycol methacrylate ($PEG_{10}MA$; 10 EG units; Sigma-Aldrich, Germany). The surfaces were exposed to UV light for 4 min. All coated surfaces, including those with only SAMs, were ultrasonicated in ethanol and rinsed thoroughly with Milli-Q water prior to use.

SPR and iSPR. Nonimaging SPR measurements of SIPC adsorption onto the different surfaces were conducted using a Biacore 3000 unit (GE Healthcare, Uppsala, Sweden). SIPC in Tris-HCl buffer (50 mM TRIS-HCl, 0.1 mg mL^{-1} SIPC, pH 8.2) was introduced over the surfaces at a flow rate of 10 mL min^{-1}. pH 8.2 was selected to approximate the conditions of footprint deposition in seawater. Each injection lasted 5 min. Binding curves from 4 flow cells were recorded for 2 replicate surfaces for all except COOH, for which 3 replicates were used. The SIPC binding, in ng mm^{-2}, was defined as the difference between the signal directly before and after the SIPC injection.

The iSPR measurements were carried out using a custom-designed instrument, presented schematically in Figure 1 and described recently elsewhere.[30] The control and image capturing software was custom-written and based on LabView (version 8, National Instruments), and the subsequent data analysis was performed within the Matlab environment (MathWorks, Inc.). Three replicate surfaces were tested for each surface chemistry, with 10 cyprids added to each surface in a ~0.5 mL drop of ASW. Once cyprids were introduced to the surface, they were induced to explore by water currents in the droplet, developed using a Pasteur pipet. At this point, image capture began and the cyprids engaged in exploratory behavior. Contact between cyprids and the surface, and deposition of footprints, were clearly visible as they occurred and a time-series of images (1 frame per second) was recorded over the course of 15 min for each surface. The cyprids were then removed. Postanalysis data treatment enabled quantification of the total number of contacts between cyprid antennules and the surface (see below for details). In addition, wavelength scans were performed to determine the SPR conditions in each pixel before and after 15 min of cyprid exploration, enabling quantitative analysis of the deposited footprints. On completion of an experiment, the average thickness of deposited footprints was estimated by measuring the difference in SPR wavelength before and after cyprid exploration.[30] In this case, a 5 × 5 pixel area from the center of three randomly chosen footprints from each surface was evaluated.

Data Analysis. Three replicate data sets for each surface were compared using one-way analysis of variance (ANOVA), or a Kruskal–Wallis test when data did not meet the requirements for parametric analysis. Pairwise comparison of data sets was carried out using Tukey's test after ANOVA (in Minitab 13) or Dunn's test after Kruskal–Wallis analysis (in Graphpad Prism).

The total numbers of cyprid-surface contacts ('touchdowns') and deposited footprints (Figure 2) were enumerated within a common region of interest (ROI), measuring 1.5 × 1.5 mm^2 and placed in the focused area of the iSPR image. Manual enumeration of the deposited footprints was performed by comparing the data from the iSPR wavelength scans before and after cyprid exploration and counting the number of light spots in the difference images (indicating a local increase in the SPR wavelength, caused by deposited material (Figure 2)). The origins of some uncertain spots with weak intensities had to be verified by reviewing the relevant sections of the touchdown image sequence. A few spots were found to be the result of adsorption of particulate material to the surface, but such events could be distinguished easily from cyprid exploration activities since the latter tended to occur suddenly and with several events in quick succession. The number of touchdowns was determined from the image sequences over a 15 min experimental period while cyprids were free to explore the surface. For each ROI, a single representative image, containing all accumulated touchdown events, was used for the manual enumeration of touchdowns. The representative images were extracted from the data sets by performing a number of operations in the image processing program ImageJ (version 1.40G), into which the complete image sequences were imported. The image processing operations served to visualize all changes in light intensity over the course of cyprid exploration (the majority of these light intensity changes were the result of cyprid activity). First, the darkest and brightest intensity values from the image sequence were determined for each pixel, and two new images showing the "darkest" and "brightest" events were constructed. The first frame of the image sequence was then subtracted from the "brightest" image to remove the background signal, which did not change during the experiment. The "darkest" image was likewise background-compensated after grayscale inversion. The new "brightest" and "darkest" images were then summed to form the final representative image, which showed the accumulated changes, both dark and bright, as bright areas against a dark background. The reason for combining a dark and a bright image was that some touchdowns appeared as dark spots, whereas others were brighter than the background, with a majority containing both bright and dark

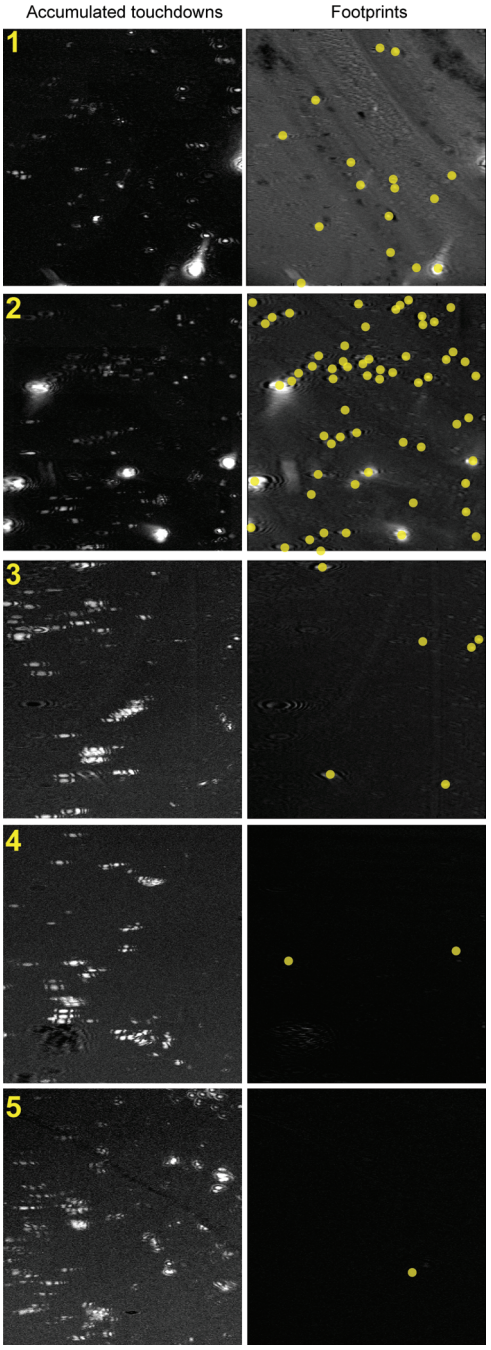

Figure 2. Example images from iSPR experiments. Accumulated touchdowns (left column) and remaining footprints (right column) are presented for one sample of each of the five investigated surface chemistries: (1) methyl, (2) carboxyl, (3) amine, (4) PEG, and (5) $PEG_{10}MA/HEMA$ (hydrogel). For clarity the deposited footprints have been marked with yellow dots. Accumulated touchdowns were, on average, approximately equal for all surfaces, whereas footprint deposition varied greatly depending on surface type.

elements. The method described above was employed because it dealt with both cases with equal fidelity.

RESULTS

Footprint Deposition Observations. Cyprids attempted exploration on all surfaces during iSPR experiments. Footprints, when deposited, were easily visible, showing up as bright spots in the iSPR field (Figure 2). In most cases, there was no doubt as to the origin of the objects identified as footprints since they were clearly the result of contact between the cyprid adhesive disk and the surface. On some occasions, however, contact between the cyprid adhesive disk and the surface did not result in the visible deposition of a footprint or, indeed, any material at all. From observation of the recorded time series and the before/after wavelengths scans it was possible to enumerate surface contacts by cyprids (termed "touchdowns") and the resulting footprint deposition on the surface (Figure 3A).

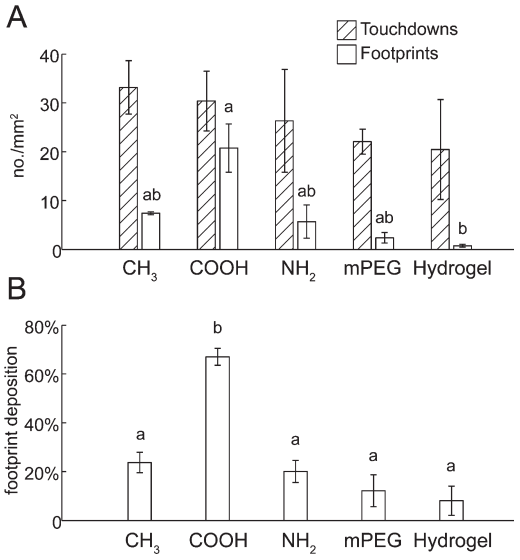

Figure 3. (A) Mean number of touchdowns made by cyprids on each surface type tested in iSPR experiments and the resulting number of footprints deposited onto each surface. (B) ratio of the data in A, giving the proportion of touchdowns that resulted in a deposited footprint for each surface type. All values are means ± the standard error of the mean. Bars that do not share a letter differ significantly at 95% alpha.

Statistical analysis using ANOVA suggested that differences in touchdowns between surface types were not significant at 95% confidence (Figure 3A; $F = 0.55$, $P = 0.706$) and, therefore, that any significant differences found between surfaces in terms of footprint deposition would likely be a result of the surface characteristics alone. In fact, significant differences in footprint deposition were observed between surfaces (Figure 3A; Kruskal–Wallis $H = 12.18$, $P = 0.016$).

To account for minor variability in the frequency of touchdowns between surfaces, footprint deposition was expressed as a proportion of touchdown events by dividing the number of persistent footprints observed on a surface by the total number of touchdowns on that surface (Figure 3B). When the data were expressed in this way, the trend remained similar to that for the raw footprint deposition data (Figure 3A). However, the only significantly different surface was COOH, which retained a larger number of footprints than any of the other surfaces (ANOVA $F = 23.91$ $P = <0.001$) as a proportion of touchdowns. The proportional data in Figure 3B provide a true reflection of the likelihood of footprint deposition as a function of total number of touchdowns on each surface. Cyprids exposed to COOH, for example, demonstrated a 67 ± 3% (SE) likelihood of depositing a footprint when contacting the surface, whereas the likelihood of deposition on other surfaces ranged from 8 to 24% (Figure 3B).

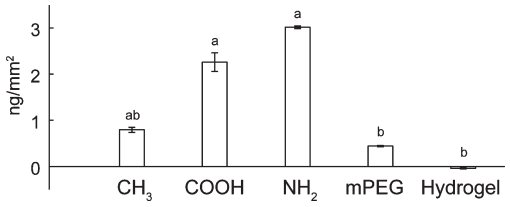

Figure 4. Binding of SIPC to five surface types (mean ± one standard error), determined using Biacore 3000 nonimaging SPR. Bars that do not share a letter differ significantly at 95% alpha.

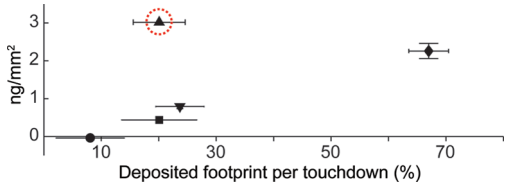

Figure 5. Relation between SIPC binding and the proportion of footprints deposited by cyprids on five experimental surfaces (± one standard error in both dimensions). Methyl = inverted triangle, carboxyl = diamond, amine = triangle, PEG = square, and $PEG_{10}MA/HEMA$ (hydrogel) = circle. Dashed circle highlights the outlying amine data point.

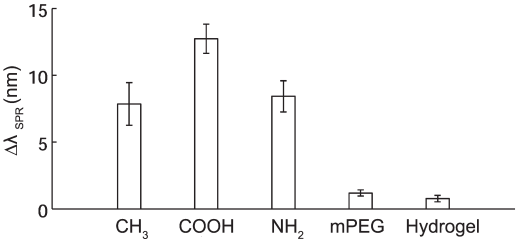

Figure 6. iSPR wavelength shift initiated by the presence of footprints on the test surfaces. This shift may be used as a relative indicator of footprint thickness on the five surfaces, with footprints on the carboxyl surface being thickest.

Adsorption of Purified SIPC. A separate experiment investigated the adsorption of purified barnacle settlement-inducing protein complex (SIPC) to the same range of test surfaces. Significant differences were observed in terms of protein adsorption to the surfaces (Figure 4; H = 38.53, P = <0.001). In particular, the PEG-containing hydrogel did not appear to bind any protein, while COOH and NH_2 showed high SIPC adsorption. Superficially, the binding of SIPC to the surfaces correlated well with footprint deposition on the same surfaces (Figure 3A, B).

Correlation of Footprint Data to SIPC Data. When the SIPC adsorption data were compared to the proportional footprint deposition data, all surfaces correlated following a linear trend with the exception of NH_2, which fell a considerable distance from the prevailing trend (Figure 5). A straight line plotted through the data for all other surfaces predicted, using a high correlation coefficient of R^2 = 0.98, that the likelihood of footprint deposition on NH_2 should be ~87% on the basis of the SIPC binding data. In fact, footprint deposition occurred at 20% ± 4.5. These data were compared to the wavelength shift changes associated with footprint deposition, which gave an indication of the relative thickness of footprints on the different surfaces. On investigation of this parameter (Figure 6), it was noted that the footprints deposited on mPEG and the hydrogel were considerably thinner than those on the other surfaces, with COOH yielding the thickest footprints. The estimates of thickness made using this method[30] conformed to those previously published by Phang et al.[13] from more laborious AFM studies of footprints on methyl SAMs.

DISCUSSION

Cyprid behavior over the course of the experiments, as quantified by number of touchdowns, was similar for all surfaces (Figure 3A). Regardless of surface chemistry, the cyprid response was to probe the surface and attempt exploration immediately when introduced into the experimental chamber. However, some surfaces, notably COOH, retained more footprints than others when subjected to the same degree of probing (Figure 3B). The frequency of footprint deposition was therefore indicative of the affinity of the adhesive material for the different surfaces tested. This conclusion was supported by similarity between the footprint deposition data (Figure 3B) and the frequency shift data in Figure 6. The similarity implies that footprint deposition was not an "all or nothing" event. In fact, the chemistry of the surface determined both the frequency of footprint deposition and "quantity" (thickness) of adsorbed material equally. Both footprint deposition data and film thickness data correlated well to SIPC binding data (Figure 5) with the exception of the amine-terminated surface. The footprints deposited onto the amine-terminated surface were also slightly thicker than would have been expected from footprint deposition data bearing this correlation in mind, whereas mPEG and the hydrogel accumulated few footprints (Figure 3B). The footprints deposited onto mPEG and the hydrogel were also very thin (no more than a trace of adsorbed material; Figure 6).

The importance of this observation is highlighted by the results of the SIPC binding experiments (Figure 4) where the NH_2 SAM stood out as being inconsistent when compared to the other surfaces using footprint deposition data in Figure 3B. Figure 5 presents SIPC binding to the range of surfaces relative to footprint deposition. Far more SIPC adsorbed to the NH_2 SAM than would have been predicted using the footprint deposition data. In other words, had SIPC binding been used as a proxy to predict attachment success for cyprids to these surfaces, it would have failed for the NH_2 SAM. Not only does this highlight the importance of investigating a specific adhesion process of interest in situ, thereby vindicating the development of a method to accomplish this, it may also provide the means for tentatively predicting the physicochemical properties of microadhesive deposits, not by conventional biochemical analysis, but by direct observation of the interaction of the adhesives with surfaces. Although the preferred approach for such characterization would usually be accumulation of sufficient adhesive material for biochemical analysis, in reality this approach has so far proven unsuccessful for cyprid adhesives, for reasons outlined in the introduction.

To summarize, the NH_2 SAM appeared to be unusual among the surfaces tested in that it bound SIPC, an adhesive component, well, but accumulated little adhesive when explored by cyprids. Further, the footprints that were deposited on the NH_2 SAM resembled those on the high-deposition COOH surface more than those on the low-deposition PEG-based surfaces in

terms of thickness (with CH_3 consistently intermediate). A complementary technique such as quartz-crystal microbalance (QCM) would be required to compare surfaces on the basis of total accumulated mass and this would be a useful and potentially informative adjunct. Extrapolating from the present data, there seems to be a characteristic of the footprint material that differs from the SIPC sufficiently to reduce the affinity of the footprint material to an NH_2-functionalized surface. This implies a significant difference, either in composition or in usage, between the footprint material in active use by a cyprid and pure SIPC passively applied to a surface for experimental purposes.

Assuming that composition is key, these data raise the possibility that purified SIPC has a net neutral surface charge, or at least that the protein surface comprises segregated positively and negatively charged domains, enabling it to bind strongly to both COOH- and NH_2-presenting surfaces (Figure 4). The natural footprint material, on the other hand, was retained predominantly on the negatively charged COOH surface, implying a dominant positive charge. A prevailing positive charge would seem to be an adaptive characteristic for a putatively adhesive material in the marine environment, where there is a preponderance of negatively charged surfaces. This natural bias toward negative surface charge is due to the formation of negatively charged electrical double layers on surfaces in alkaline media (e.g., seawater[40]). Indeed, other sessile marine organisms such as blue mussels (*Mytilus edulis*) use adhesive complexes with abundant arginine and/or lysine residues, resulting in high (basic) protein pI values and a contribution to adhesion by the positive surface charge on the adhesive.[41] This hypothesis would suggest that the difference in footprint deposition between COOH and all other surfaces (Figure 3B) might be due to electrostatic attraction of the footprint material to the negatively charged surface chemistry. The polarity of the footprint material and its adaptive significance has been speculated on previously[23,14] and hopefully it will one day be possible to validate these predictions in isoelectric focusing experiments.

There is, of course, a more pragmatic possible explanation for the trends observed here. For SIPC binding we observed the adsorption of a molecule to different surfaces; a process governed entirely by physical principles. In the experiments using live cyprids, however, we cannot exclude the possibility that there is an element of "choice" in the deposition of adhesive to surfaces during exploration. Again, this only reinforces the importance of exercising caution before extrapolating from molecular-scale proof-of-concept experiments to organism-scale real-world applications. The ultimate implication of these data, however, is that the process of cyprid temporary attachment to well-characterized surfaces could potentially reduce to a thermodynamic balance of forces in the surface/footprint/adhesive disk system (See ref 42 for an early application of this hypothesis). For surfaces where forces between the surface chemistry and the footprint protein are weak, the likelihood is that the footprint material will remain on the adhesive disk rather than the surface on detachment, implying also that forces between the surface and the footprint are not sufficiently strong to allow surface exploration and settlement. On the other hand, on a surface where the footprint material binds strongly, one would expect failure to occur at the footprint/antennular disk interface or within the footprint material, leaving some material on the surface and some on the disk (i.e., cohesive failure).

Regarding the method itself, the iSPR technique is presently only able to quantify organism-surface contact and footprint deposition in combination with a manual enumeration method. The image-processing protocols used here led to a loss of temporal information in the case of touchdown quantification which was compensated for by surveying the captured video sequences when necessary. Clearly, however, further development and automation of the quantification method would be necessary to realize the full potential of the iSPR technique in this application. For instance, there is currently no distinction made between touchdowns caused by cyprids moving rapidly and those that were stationary or moving more slowly. Since it is possible, and perhaps likely, that footprint deposition would also be a function of cyprid activity, it will be necessary in the future to quantify cyprid activity using a remote tracking method[43,44] during experiments. Additionally, an algorithm enabling automatic enumeration of touchdowns and footprint deposition would make data processing quicker, less labor-intensive, and more reproducible.

In terms of its potential use, the imaging SPR method may be used throughout antibiofouling research to observe directly the interactions of microfoulers with surfaces and to quantify the success rate of adhesion events with confidence. In combination with other methods, as briefly demonstrated here, the technique may allow broad-scale assumptions to be made regarding the characteristics and behavior of adhesives in contact with surfaces when more refined biochemical analyses of those materials are impossible or impractical. For those working in antibiofouling research, these data will provide encouragement that the philosophy of nonfouling coatings design, drawing on PEG chemistry,[38,45] zwitterions,[46−48] and fluoropolymers[49,50] may be a highly productive avenue of research. The hydrogel used here retained only 8 ± 6% of footprints (Figure 3B), implying that in ∼90% of cases, cyprids would not attach strongly enough to engage in permanent settlement, even if they were stimulated to do so. If the successful proportion can be reduced still further and the surfaces remain stable on exposure to seawater, nonfouling surface technology may be a viable replacement for the current generation of biocidal marine paints.[51]

AUTHOR INFORMATION

Corresponding Author

*E-mail: a.s.clare@ncl.ac.uk.

ACKNOWLEDGMENT

The authors acknowledge financial support from the AMBIO project (NMP-CT-2005-011827), funded by the European Commission's sixth Framework Programme. A.S.C. further acknowledges the U.S. Office of Naval Research (Grant N-00014-08-11240). The views expressed in this work reflect only those of the authors, and the European Commission is not liable for any use that may be made of the information contained herein. Olof Andersson and Bo Liedberg acknowledge financial support from the Swedish Research Council (VR). Special thanks to Rasband, W.S., ImageJ, U.S. National Institutes of Health, Bethesda, Maryland, USA, http://rsb.info.nih.gov/ij/, 1997−2009.

REFERENCES

(1) Federle, W. *J Exp. Biol.* **2006**, *209*, 2611–2621.

(2) Huber, G.; Mantz, H.; Spolenak, R.; Mecke, K.; Jacobs, K.; Gorb, S. N.; Arzt, E. *Proc. Natl. Acad. Sci. U.S.A.* **2005**, *102*, 16293–16295.

(3) Kamino, K. In *Biological Adhesives*; Smith, A. M., Callow, J. A., Eds.; Springer-Verlag: Heidelberg. Germany, 2006; pp 145−166.
(4) Stewart, R. J.; Weaver, J. C.; Morse, D. E.; Waite, J. H. *J. Exp. Biol.* **2004**, *207*, 4727–4734.
(5) Lin, Q.; Gourdon, D.; Sun, C.; Holten-Andersen, N.; Anderson, T. H.; Waite, J. H.; Israelachvili, J. N. *Proc. Natl. Acad. Sci. U.S.A.* **2007**, *104*, 3782–3786.
(6) Yule, A. B.; Walker, G. *J. Mar. Biol. Assoc. U.K.* **1985**, *65*, 707–712.
(7) Clare, A. S.; Freet, R. K.; McClary, M. J. *J. Mar. Biol. Assoc. U.K.* **1994**, *74*, 243–250.
(8) Aldred, N.; Wills, T.; Williams, D. N.; Clare, A. S. *J. R. Soc. Interface* **2007**, *4*, 1159–1167.
(9) Callow, J. A.; Crawford, S. A.; Higgins, M. J.; Mulvaney, P.; Wetherbee, R. *Planta* **2000**, *211*, 641–647.
(10) Callow, J. A.; Callow, M. E.; Ista, L. K.; Lopez, G.; Chaudhury, M. K. *J. R. Soc. Interface* **2005**, *2*, 319–325.
(11) Phang, I. Y.; Aldred, N.; Clare, A. S.; Callow, J. A.; Vancso, G. J. *Biofouling* **2006**, *22*, 245–250.
(12) Aldred, N.; Phang, I. Y.; Conlan, S. L.; Clare, A. S.; Vancso, G. J. *Biofouling* **2008**, *24*, 97–107.
(13) Phang, I. Y.; Aldred, N.; Clare, A. S.; Vancso, G. J. *J. R. Soc. Interface* **2008**, *5*, 397–401.
(14) Phang, I. Y.; Aldred, N.; Ling, X. Y.; Tomczak, N.; Huskens, J.; Clare, A. S.; Vancso, G. J. *J. Adhes.* **2009**, *85*, 616–630.
(15) Phang, I. Y.; Aldred, N.; Ling, X. Y.; Huskens, J.; Clare, A. S.; Vancso, G. J. *J. R. Soc. Interface* **2010**, *7*, 285–296.
(16) Higgins, M. J.; Molino, P.; Mulvaney, P.; Wetherbee, R. *J. Phycol.* **2003**, *39*, 1181–1193.
(17) Walker, G. C.; Sun, Y. J.; Guo, S. L.; Finlay, J. A.; Callow, M. E.; Callow, J. A. *J. Adhes.* **2005**, *81*, 1101–1118.
(18) Dugdale, T. M.; Dagastine, R.; Chiovitti, A.; Mulvaney, P; Wetherbee, R. *Biophys. J.* **2005**, *89*, 4252–4260.
(19) Dugdale, T. M.; Dagastine, R.; Chiovitti, A.; Mulvaney, P.; Wetherbee, R. *Biophys. J.* **2006**, *90*, 2987–2993.
(20) Dugdale, T. M.; Willis, A.; Wetherbee, R. *Biophys. J.* **2006**, *90*, L58–L60.
(21) Schmidt, M.; Cavaco, A.; Gierlinger, N.; Aldred, N.; Fratzl, P.; Grunze, M.; Clare, A. S. *J. Adhes.* **2009**, *85*, 135–151.
(22) Petrone, L.; Ragg, N. L. C.; McQuillan, A. J. *Biofouling* **2008**, *24*, 405–413.
(23) Aldred, N.; Clare, A. S. In *Functional Surfaces in Biology Volume 2: Adhesion Related Phenomena*; Gorb, S., Ed.; Springer: Heidelberg, Germany, 2009; pp 43−66.
(24) Aldred, N.; Clare, A. S. *Biofouling* **2008**, *24*, 351–363.
(25) Lagersson, N. C.; Høeg, J. T. *Mar. Biol.* **2002**, *141*, 513–526.
(26) Nott, J. A.; Foster, B. A. *Philos. Trans. R. Soc., Ser. B* **1969**, *256*, 115–134.
(27) Yule, A. B.; Walker, G. In *Barnacle Biology*; Southward, A. J., Ed.; Crustacean Issues;A.A. Balkema: Rotterdam, Germany, 1987; Vol. 5, pp 389−402.
(28) Matsumura, K.; Nagano, M.; Kato-Yoshinaga, Y.; Yamazaki, M.; Clare, A. S.; Fusetani, N. *Proc. R. Soc. London, Ser. B* **1998**, *265*, 1825–1830.
(29) Dreanno, C.; Kirby, R. R.; Clare, A. S. *Biol. Lett.* **2006**, *2*, 423–425.
(30) Andersson, O.; Ekblad, T.; Aldred, N.; Clare, A. S.; Liedberg, B. *Biointerphases* **2009**, *4*, 65–68.
(31) Dreanno, C.; Matsumura, K.; Dohmae, N.; Takio, K.; Hirota, H.; Kirby, R. R.; Clare, A. S. *Proc. Natl. Acad. Sci. U.S.A.* **2006**, *103*, 14396–14401.
(32) Dreanno, C.; Kirby, R. R.; Clare, A. S. *Proc. R. Soc. London, Ser. B* **2006**, *273*, 2721–2728.
(33) Clare, A. S. In *Chemical Communication in Crustaceans*; Breithaupt, T; Thiel, M, Eds.; Springer: New York, 2011; pp 431−450.
(34) Nakano, M.; Shen, J. R.; Kamino, K. *Biomacromolecules* **2007**, *8*, 1830–1835.
(35) Gorb, S. N. *Philos. Trans. R. Soc., Ser. A* **2008**, *366*, 1557–1574.
(36) Nosonovsky, M.; Bhushan, B. *Philos. Trans. R. Soc., Ser. A* **2009**, *367*, 1511–1539.
(37) Ralston, E.; Swain, G. *Bioinsp. Biomim.* **2009**, *4*, 1–9.
(38) Ekblad, T.; Bergström, G.; Ederth, T.; Conlan, S. L.; Mutton, R. J.; Clare, A. S.; Wang, S.; Liu, Y.; Zhao, Q.; D'Souza, F.; Donnelly, G. T.; Willemsen, P. R.; Pettitt, M. E.; Callow, M. E.; Callow, J. A.; Liedberg, B. *Biomacromolecules* **2008**, *9*, 2775–2783.
(39) Larsson, A.; Ekblad, T.; Andersson, O.; Liedberg, B. *Biomacromolecules* **2007**, *8*, 287–295.
(40) Rhodes, M. *Introduction to Particle Technology*, 2nd ed.; John Wiley and Sons: Chichester, U.K., 2008.
(41) Zhao, H.; Robertson, N. B.; Jewhurst, S. A.; Waite, J. H. *J. Biol. Chem.* **2006**, *281*, 26150–29158.
(42) Crisp, D. J.; Walker, G.; Young, G. A.; Yule, A. B. *J. Colloid Interface Sci.* **1985**, *104*, 40–50.
(43) Marechal, J. P.; Hellio, C.; Sebire, M.; Clare, A. S. *Biofouling* **2004**, *20*, 211–217.
(44) Aldred, N; Li, G; Gao, Y; Clare, A. S; Jiang, S. *Biofouling* **2010**, *26*, 673–683.
(45) Schilp, S.; Rosenhahn, A.; Pettitt, M.; Bowen, J.; Callow, M.; Callow, J. A.; Grunze, M. *Langmuir* **2009**, *25*, 10077–10082.
(46) Ladd, J.; Zhang, Z.; Chen, S. F.; Hower, J. C.; Jiang, S. Y. *Biomacromolecules* **2008**, *9*, 1357–1361.
(47) Yang, W.; Chen, S.; Cheng, G.; Vaisocherová, H.; Xue, H.; Li, W.; Zhang, J.; Jiang, S. Y. *Langmuir* **2008**, *24*, 9211–9214.
(48) Cheng, G.; Li, G.; Xue, H.; Chen, S.; Zhang, Z.; Bryers, J. D.; Jiang, S. Y. *Biomaterials* **2009**, *30*, 5234–5240.
(49) Cheng, G.; Zhang, Z.; Chen, S.; Bryers, J. D.; Jiang, S. Y. *Biomaterials* **2007**, *28*, 4192–4199.
(50) Bartels, J. W; Cheng, C.; Powell, K. T.; Xu, J.; Wooley, K. L. *Macromol. Chem. Phys.* **2007**, *208*, 1676–1687.
(51) Omae, I. *Chem. Rev.* **2003**, *102*, 3431–3448.